

Dose Rate Effects in Linear Bipolar Transistors

Allan Johnston, *Fellow, IEEE*, Randall Swimm, R. D. Harris, and Dennis Thorbourn

Abstract – Dose rate effects are examined in linear bipolar transistors at high and low dose rates. At high dose rates, approximately 50% of the damage anneals at room temperature, even though these devices exhibit enhanced damage at low dose rate. The unexpected recovery of a significant fraction of the damage after tests at high dose rate requires changes in existing test standards. Tests at low temperature with a one-second radiation pulse width show that damage continues to increase for more than 3000 seconds afterward, consistent with predictions of the CTRW model for oxides with a thickness of 700 nm.

I. INTRODUCTION

In mainstream linear integrated circuits, one of the first processing steps is to grow a thick oxide that allows n-type “islands” to be formed within the epitaxial layer, using deep boron diffusions through openings in the oxide. That oxide (further modified in subsequent processing steps) remains over the emitter-base junction of lateral pnp and substrate pnp transistors, but not in npn transistors. The oxide thickness is between 700 and 1300 nm, depending on the specific process.

Many devices that use this process exhibit enhanced low dose radiation sensitivity (ELDRS), which causes significantly more damage to occur at the low dose rates in space compared to damage in high-dose rate tests. Although this effect was first observed 20 years ago [1], it is still not fully understood.

This paper investigates the effect of irradiation at different dose rates in more detail, using a combination of computer modeling and experimentation. The objective of the work is to compare the time response of damage in bipolar structures with previous work on MOS devices, and to provide additional insight into the mechanisms for charge buildup.

II. APPROACH

A. Device Selected for Study

LM111 comparators from National Semiconductor were used for initial work; they were JANTX qualified, but unhardened. Measurements of input bias current have been used in several previous studies of low-dose rate effects in this device [2-6].

A simplified input schematic of this device is shown in Fig. 1. Although the second stage npn transistors affect the loading on the input pnp transistors, it is possible to eliminate that interaction by applying a differential

The authors are with the Jet Propulsion Laboratory, California Institute of Technology, Pasadena, CA, USA. E-mail: allan.h.johnston@jpl.nasa.gov; randall.t.swimm@jpl.nasa.gov; dennis.thorbourn@jpl.nasa.gov.

The research in this paper was carried out at the Jet Propulsion Laboratory, California Institute of Technology, under contract with the National Aeronautics and Space Administration (NASA); © 2011, California Institute of Technology, government sponsorship acknowledged.

voltage of ~ 200 mV between the input terminals. This diverts nearly all the current to one npn transistor, effectively isolating the input pnp transistor that drives the other npn device. With this approach, the input current of the pnp transistor with the lowest input voltage depends only on the gain of the pnp device as long as the internal current sources are unaffected. This measurement approach also removes the nonlinearity at high total dose levels that is caused by the effects of npn loading.

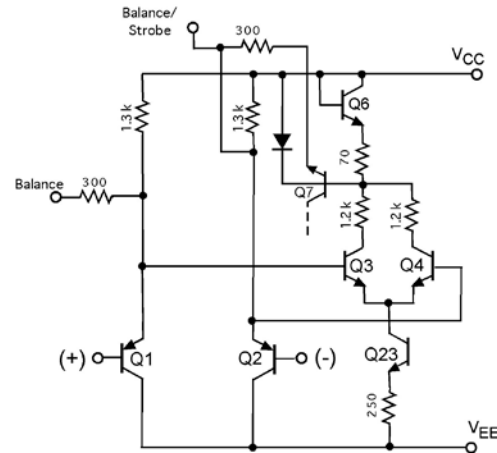


Fig. 1. Simplified schematic diagram of the LM111 input stage.

Additional tests were done on OP27 operational amplifiers, manufactured by Analog Devices. That amplifier used a compensated input stage, shown in simplified form in Fig. 2; this complicates the interpretation of changes in bias current compared to the LM111. The main purpose of including the OP27 was to compare post-irradiation annealing with that of the LM111 to ensure that the basic features of annealing were similar for the two manufacturers.

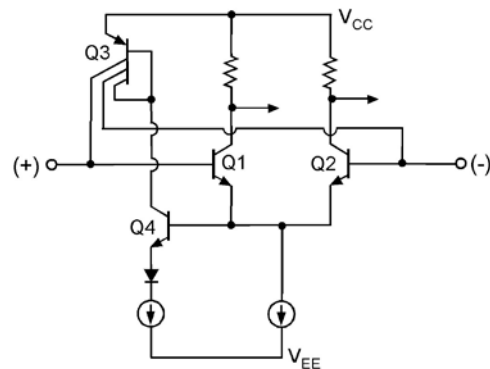


Fig. 2. Simplified diagram of the input stage of the OP27 operational amplifier.

B. Special Pulsed Measurements

A pulsed measurement technique was used for measurements on devices irradiated with the JPL Dynamitron that allowed the input bias current to be measured during a single 20 ms time interval, using a symmetrical pulse source to apply power, triggering a digital voltmeter with a 16.7 ms integration time shortly after power was applied. This was done to limit the time period during which bias was applied; it was short enough compared to irradiation times to essentially eliminate the effects of applied bias.

A local buffer amplifier was used on the test card, shielding the buffer from the beam with an aluminum shield. Currents as low as 1 nA could be measured, with an accuracy of ± 0.5 nA.

III. TEST RESULTS AT ROOM TEMPERATURE

A. Low Dose Rate Baseline Data

Cobalt-60 gamma rays were used to obtain baseline radiation data, serving as a reference point for other test results. The dose rate used for these tests was 0.005 rad(SiO₂)/s. Figure 3 shows the mean change in input bias current for biased and unbiased LM111 devices, along with the 8.5 krad(SiO₂) reference point for comparison with later irradiations at higher dose rates. Note that the damage is nearly linear with dose up to that reference level, and that there is a substantial difference for the two bias conditions.

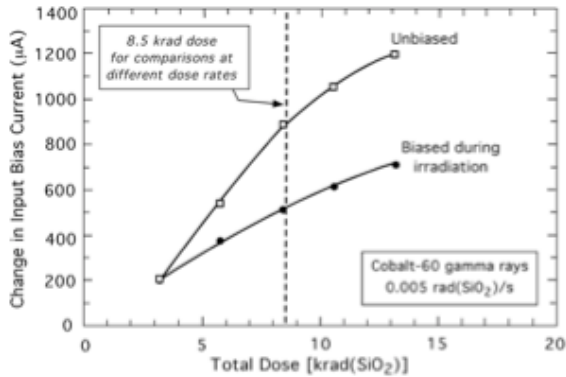


Fig. 3. Change in input bias current for biased and unbiased LM111 circuits at a dose rate of 5 mrad(SiO₂)/s. The vertical line shows the total dose used for comparison with high-energy electron tests at higher dose rates.

Similar low dose rate test results for the OP27 are shown in Fig. 4. Due to the current compensated design of the input stage, changes in input current are initially very low, and only become significant at higher radiation levels when the damage is sufficiently high to degrade the input current compensation circuit [7].

B. Tests at Higher Dose Rates with Electrons

The JPL Dynamitron was used for experiments at higher dose rates, using 1.3 MeV electrons. Those irradiations were done in vacuum. Several tests were

done at different dose rates. The comparisons were made at constant dose, 8.5 krad(SiO₂), within the linear damage range for this device. Table 1 shows the conditions used for tests of the LM111. Tests of the OP27 were only done under one condition, 40 krad(SiO₂) at 100 rad(SiO₂)/s, a four-second irradiation time. A higher total dose was needed for that device because of the nonlinear dependence of changes in input bias current with total dose.

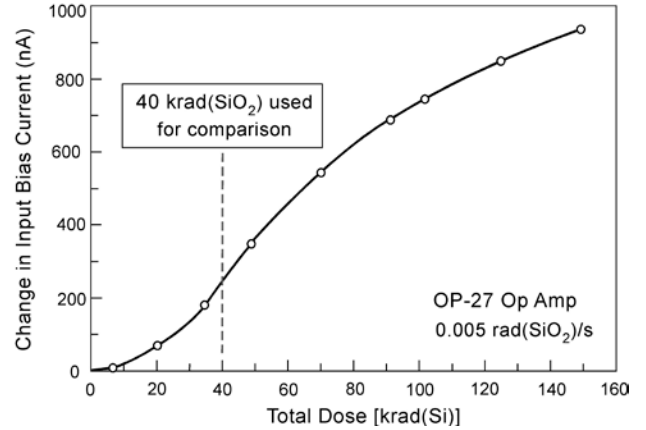


Fig. 4. Dependence of input bias current on total dose for the OP27 op-amp at low dose rate. A total dose of 40 krad(SiO₂) was used to compare results at different dose rates.

Table 1
LM111 Test Conditions for Irradiations to 8.5 krad(SiO₂)

Dose Rate [rad(SiO ₂)/s]	Irradiation Time (seconds)	Bias Conditions
10,000	0.84	Unbiased
1,032	8.3	Unbiased
101	84	Unbiased
2.4	3500	Biased and Unbiased

Electrical tests were made periodically after each irradiation to approximately 2×10^6 s in order to determine damage stability after irradiation. For time periods up to $\sim 10^4$ s, measurements were made by biasing the device with a single 20 ms, pulse, as described above. For time periods $> 50,000$ s, measurements were made with an Agilent 4156 parameter analyzer, applying power to the device for about 1.5 s.

LM111 Comparator

Despite the high sensitivity of the LM111 to the ELDRS effect, a significant fraction of the damage was found to anneal at room temperature after irradiation. Figure 5 compares post-irradiation measurements for different dose rates, along with the damage that was observed during the low dose rate tests. Annealing was done without applied bias (all pins at ground). Although the irradiation times varied, the total dose at the end of each run was 8.5 krad(SiO₂). Measurements were done

at the end of each run, without taking the irradiation time into account. This decreases the recovery at shorter times, which is particularly evident for the 2.4 rad(SiO₂)/s case.

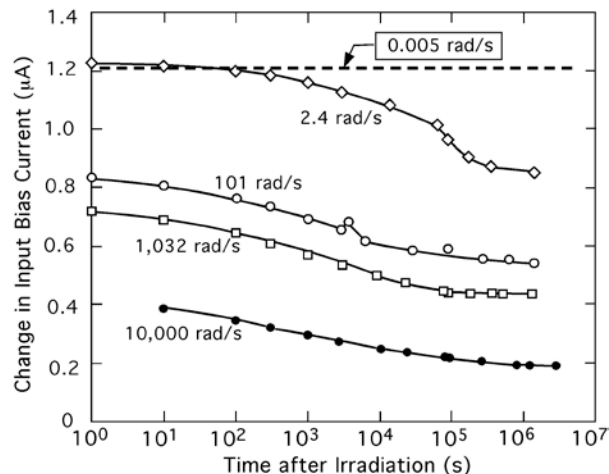


Fig. 5. Annealing results for samples irradiated without applied bias to 8.5 krad(SiO₂). The dashed line shows cobalt-60 results at 0.005 rad(SiO₂)/s.

At 100 rad(SiO₂)/s, the nominal dose rate used for “high dose rate” testing, the damage is about 20% lower for measurements made 20 minutes after irradiation compared to the damage that is present just after the irradiation. The relatively rapid recovery of damage after irradiation is an important interference factor for measurements at high dose rate. Current testing standards allow up to two hours between successive irradiations. For a part with relatively rapid recovery, such as the LM111 in this study, the time interval between irradiations needs to be controlled more carefully in order to provide consistent measurement results. If we normalize the damage at short times to the stable damage at long times, it levels out at dose rates of 100 rad(SiO₂) or lower (Fig. 6).

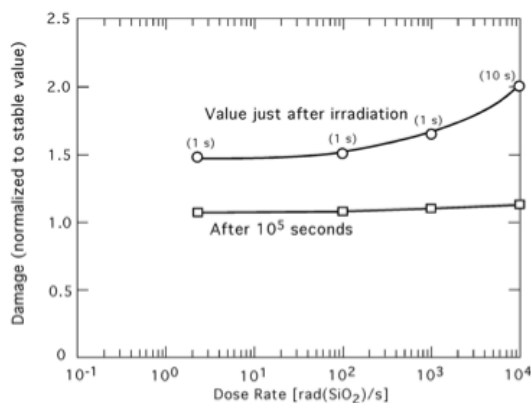


Fig. 6. Normalized damage at short times and at 10⁵ seconds after irradiation for devices irradiated to 8.5 krad(SiO₂) at different dose rates. One-third to one-half of the initial damage anneals at room temperature.

Normalized damage 10⁵ seconds after irradiation is also shown; nearly all the damage that can potentially recover has recovered at that time. The time for half the damage to recover is about 1500 seconds; this is addressed in more detail in the discussion section.

Initial and final values for ΔI_b are shown in Fig. 7, adjusting the initial value for the 2.4 rad(SiO₂)/s case upward by 5% to account for annealing during the long irradiation time. Stable and recoverable damage both increase as the dose rate is reduced.

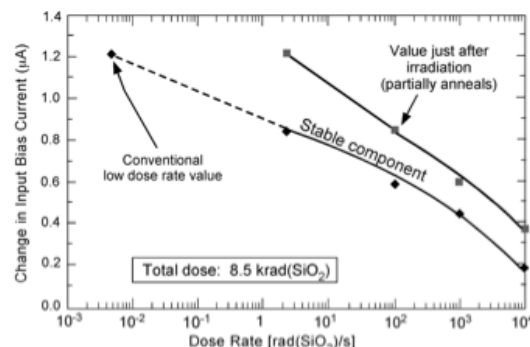


Fig. 7. Post-irradiation and long-term values for ΔI_b after irradiation to 8.5 krad(SiO₂) at various rates. Devices were irradiated with all pins at ground (other than the 20 ms time required for electrical measurements).

Biased and unbiased irradiations were done (on separate samples) at a dose rate of 2.4 rad(SiO₂)/s. Those results are shown in Fig 8. Less damage occurred in the biased samples, but the annealing results were roughly the same (unbiased samples remained unbiased during annealing).

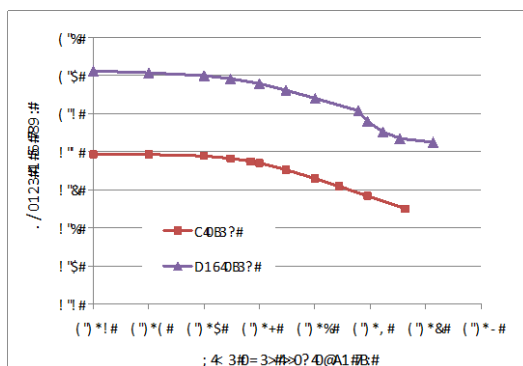


Fig. 8. Results for biased and unbiased LM111 samples, using a dose rate of 2.4 rad(SiO₂)/s.

OP27 Op-Amp

A more limited set of tests was done on the OP27 op-amp samples. Tests with the Dynamitron were done at a dose rate of 100 rad(SiO₂)/s, to a total dose of 40 krad(SiO₂). Input bias current was measured using the same 20 ms pulsed method. Test results for that circuit are shown in Fig. 9; results for the LM111 are also included in the figure for comparison.

It is more difficult to assess recovery in the OP27 because of the nonlinear dependence of changes in input bias current compared to the linear damage of the LM111. Nevertheless, we can conclude from these results that substantial annealing takes place for that device after irradiation, demonstrating that the recovery we observe after irradiation for the LM111 is also exhibited in parts produced on similar linear processes from other manufacturers that are also sensitive to the ELDRS effect.

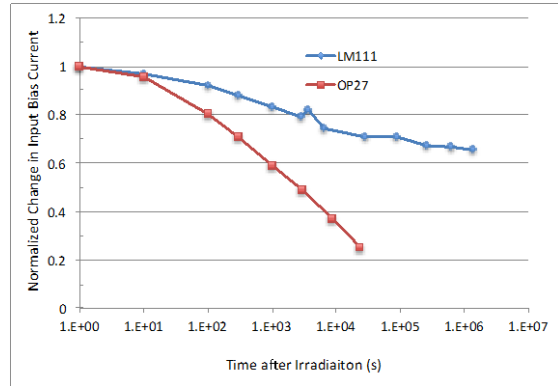


Fig. 9. Annealing results for the OP27 op-amp after irradiation to 40 krad (SiO_2) at a dose rate of 100 rad(SiO_2)/s.

IV. TESTS AT OTHER TEMPERATURES

A series of radiation tests with a one second irradiation time was done on the LM111 comparator at a dose rate of 8.5×10^4 rad(SiO_2)/s (this provided a total dose of 8.5 krad(SiO_2) in one second). A thermoelectric cooler was used to maintain the temperature during irradiation, as well as for extended periods afterwards. Results for four different temperatures are shown in Fig. 10. The low temperature tests have a different response than the tests at room temperature and above. At 45 °C there is about 15% more damage compared to room temperature. The damage at both temperatures anneals, with similar slopes, continuing to about 10^6 seconds. About 45% of the damage appears to be stable after that time, but there is more residual damage for the higher temperature, consistent with the higher damage observed just after the irradiation.

At 0 °C and -25°C, damage continues to build up after the irradiation pulse. At the lower temperature, this build-up time persists for about 3000 seconds, suggesting that holes generated during the irradiation are gradually accumulating at the interface region, due to slow hole transport in thick oxides. This is consistent with the highly dispersive CTRW model that was developed during the 1980's for MOS gate oxides, and is discussed in more detail in the next section.

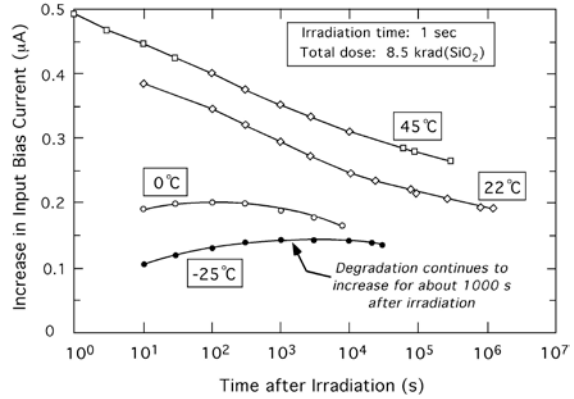


Fig. 10. LM111 tests at various temperatures. The irradiations were done at the same total dose for all temperatures.

V. DISCUSSION

A. Recombination

Two recombination processes need to be considered in the bipolar oxide problem. First, there is some probability that an electron-hole pair may recombine just after it is created, which is typically described by the hole yield function [8]. This is affected by the magnitude of the electric field as well as the electron-hole pair density. In bipolar oxides the electric field is usually low, < 0.3 MV/cm, and lower still for irradiations that are done without bias, where the internal fields are established by differences in work functions. For such low fields, the yield function for electrons or gamma rays is < 0.3 .

After separation, the electron is quickly transported away, but hole transport proceeds slowly. A background level of electrons is present during the time that the radiation is applied; the electron-hole density at the highest dose rates used in our experiments is about 10^{17} cm^{-3} . The second recombination process involves recombination of holes with the steady-state electron density during irradiation. Holes are subject to this recombination process until they are trapped, or until the irradiation ceases.

B. Annealing

The conventional view of parts that are sensitive to ELDRS is that little or no annealing takes place (at room temperature); at first glance, this would appear to be a necessary condition in order for more damage to take place at low dose rate, where much longer irradiation times are involved. However, tests at different dose rates show that there are stable and recoverable components to the overall damage, even at room temperature, and that their ratio is only weakly dependent on the dose rate used for irradiation. This implies that annealing is not directly related to the ELDRS effect; more damage takes place for both the stable and recoverable damage components at low dose rate.

This is important when we interpret test results. MilStd 1019 allows up to two hours between successive

irradiations. For the particular device technology used in the LM111, about 20% of the damage recovers after one hour when the irradiation is done at 100 rad(SiO₂)/s. Much longer times are required to do a series of successive irradiation, which is the typically done for characterization at high dose rate. Consequently, 30 to 40% of the damage is likely to recover during the course of an experimental run at high dose rate unless the time between irradiation and measurement is carefully controlled.

Annealing of the recoverable component appears to fit the log(t) relationship [9] that applies to annealing of trapped holes MOS devices reasonably well. Equation 1 shows this relationship with appropriate modifications for input bias current

$$\Delta I_b(t) = \frac{A \log(t) + C}{\gamma_o} \quad (1)$$

where $\Delta I_b(t)$ is the change in input bias current after an annealing time t , γ_o is the total dose after irradiation, and A and C are constants that are fitted to the data. The results of two of the irradiations are fitted with this equation in Fig. 11; the fit is reasonable out to $\sim 10^6$ seconds, when annealing saturates. The slopes are nearly the same for the two different dose rates.

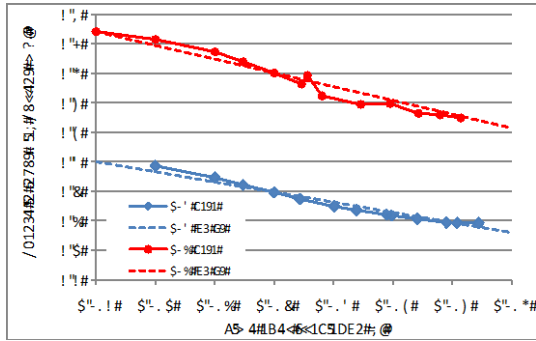


Fig. 11. Fit of Eq. 1 to experimental results at 10,000 and 101 rad(SiO₂)/s; the irradiations and anneal were done at room temperature.

Similar fits were obtained for the other dose rates. The time for 50% of the recovery to occur was about 1500 seconds for all four dose rates. The similarity of this result to older threshold voltage data implies that trapped holes are annealing.

B. Low Temperature Radiation Test Results

Time Dependence

At the two lower temperatures – 0 °C and -25 °C – damage accumulates well after the 1-s radiation pulse has ended. This is consistent with the long time required for hole transport in thick oxides at low temperature [10, 11].

If we assume the CTRW model [12] applies, we can scale older results for the effect of temperature (obtained

with capacitor tests on 96.5 nm oxides) by a factor of t_{ox}^4 , consistent with the assumption that the parameter α in the CTRW model is 0.25. The scaled time, $t_{50\%}$, and the time required for 75% of the charge to be transported are shown in Table 2. The 75% time interval is in reasonable agreement with the delayed time for transport shown in Fig. 10 at the two lower temperatures; those estimates are shown in the last column.

Table 2. Normalized Time and Time for 75% of the Holes to Transport from the CTRW Model (based on older data with 96.5 nm, and $\alpha = 0.25$)

T (°C)	$t_{(50\%)}$	$t_{(75\%)}$	Estimated from Data
-25	13	1334	2000
0	2.3	233	170
22	0.5	50	-
45	0.1	10	-
65	0.025	2.5	-

These results imply that there is a direct connection between the older results from capacitor studies and damage in bipolar transistor structures. Despite the absence of a conductor at the outer boundary of the oxide over the emitter-base and collector-base junctions, it appears that charge is collected over the entire thickness of the oxide. This allows us to relate the older oxide studies to the more complex structure of bipolar oxides.

The result in Fig. 10 show that annealing is nearly identical for irradiations at 22 °C and 45 °C. Although annealing was examined over shorter time periods for the irradiations that were done at low temperature, the data generally support the assumption that annealing occurs at the same rate for those temperatures as well. This is consistent with the assumption of a tunneling front for the annealing of trapped holes; tunneling is independent of temperature.

With that assumption, it is possible to extrapolate experimental observations at longer times to the damage at a time period of one second, recognizing that it is not possible to actually measure that much damage at lower temperatures because of the slower hole transport.

Figure 12 compares extrapolated values for all four temperature cases, using the annealing time constant from the 45 °C case. If we examine the data in this way, it appears that the difference in actual damage at short times is only about 30%. Note that the extrapolated values at 0 and -25 °C are nearly identical. This is a key finding, which will be explained in Section IV-E.

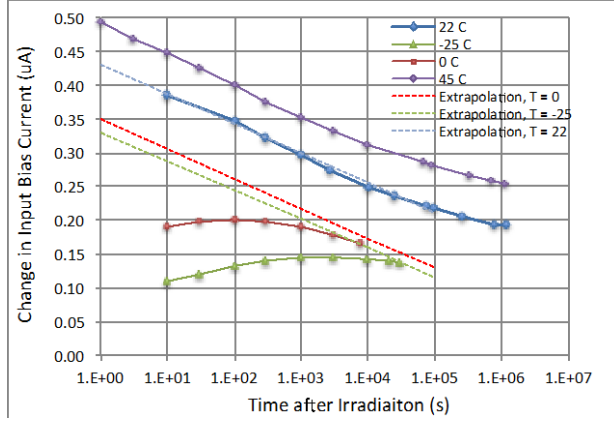


Fig. 12. Data of Fig. 10 including extrapolations of the damage to an equivalent time of one second after irradiation.

D. Oxide Geometry and Electric Field

Electric fields in bipolar screening oxides are highly non-uniform. The fields are low, reducing charge yield, except near junction fringing fields and contacts. Although we did all of our experimental work without bias (all pins at ground), it is useful to examine the magnitude and direction of the fields within the oxides, particularly because damage in these types of bipolar structures is usually more severe without bias.

We used the Synopsys device analysis program to determine the electric fields within the oxides on the surface of npn and npn transistors. An example is shown in Fig. 13 for the emitter-base fringing fields of an npn transistor. Note the complex nature of the field lines.

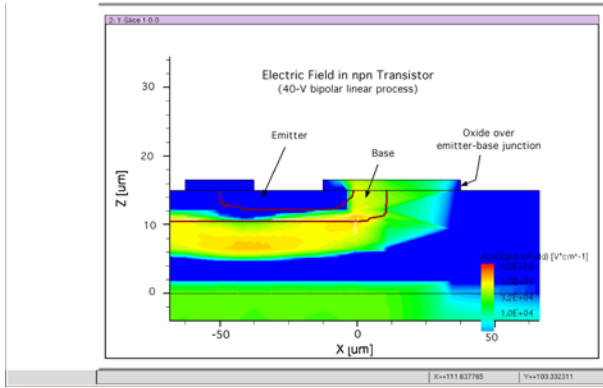


Fig. 13. Magnitude of the electric field in the gate region over the npn transistor, calculated using the Synopsys device analysis program.

E. Mechanisms for ELDRS

Current Point of View

As summarized in the review article by Pease, *et al.* [13], mechanisms for ELDRS can be divided into three categories: space-charge models, bimolecular process models, and binary rate models. All three models have

been applied to different devices and experiments (such as electron trapping in [14]), and remain viable explanations.

Older studies on gate oxides have shown that charge transport can be described by a hopping model that is highly dispersive, the continuous time, random walk (CTRW) model [11]. This process is highly dispersive; it actually spans more than twelve decades of time. If we use a characteristic time, t_{50} , for 50% of the holes to be transported, it takes 450 times longer for transport of the next 25% of the generated holes, and even longer time periods for the remaining 25%. Thus, this transport mechanism results in much longer time periods before equilibrium conditions are reached, but relatively short time periods for transport of the first half of the charge.

This dispersive transport may affect annealing results, particularly during short irradiation times, because a significant fraction of the holes may still remain to be transported. Residual holes – still in transport – may explain the larger fraction of unstable damage that was observed at high dose rate in our work (Fig. 4).

Implications of the Present Work

The low temperature results show that hole transport persists long after the end of the radiation when a one-second pulse is used. At -25°C , damage continues to increase out to approximately 3,000 seconds. We will assume that very little transport takes place during the one-second pulse at -25°C , and that the reduction in damage at low temperature, compared to room temperature, is due to recombination between the excess electrons generated during the pulse and holes that are effectively immobile during the time of the irradiation. The holes gradually build up as the irradiation proceeds, while the electrons, which have high mobility, have essentially a constant population density during the time of the irradiation.

The difference in extrapolated damage at low temperature and higher temperatures can be used to estimate the capture cross section for electrons during the pulse, assuming that all the holes remain in place at the lowest temperature. The electron-hole pair density at $10^4 \text{ rad}(\text{SiO}_2)/\text{s}$ can be determined from the generation constant for SiO_2 :

$$\Delta n = G * D = 8.1 \times 10^{16} e^{-h} \text{ pairs} / \text{cm}^3 - \text{s} \quad (2)$$

The observed damage is 30% lower, implying that about 1/3 of the holes created during the pulse recombine. The recombination rate, η , is then

$$\eta = 8.32 \times 10^{-18} \text{ cm}^3 - \text{s} \quad (3)$$

The dependence of damage on dose rate can then be determined from the highly dispersive transport properties of the CTRW model, shown in Fig. 14. If we assume that the number of holes lost through recombination with excess electrons produced during

irradiation, then the number of holes that survive radiation-induced recombination during a steady-state irradiation that persists for a time t is

$$\Delta n_{surv} = \Delta n(1 - \eta t_{rad}) \quad (4)$$

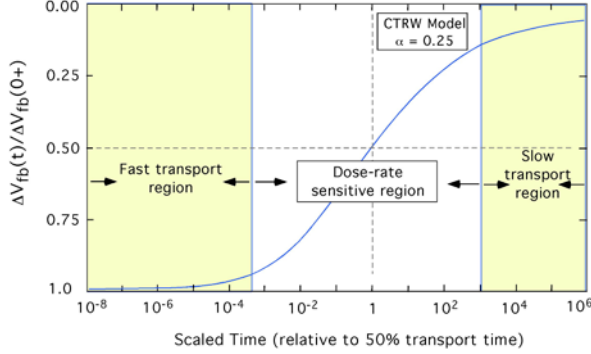


Fig. 14. CTRW model showing the three time regimes for hole transport. The ELDRS effect occurs when recombination from the sea of electrons during the pulse is sufficiently high to intercept a significant fraction of the holes before they are transported to the interface region, where they can be trapped.

First, consider two limiting cases, noting that the $t_{50\%}$ reference time, which we shall define as τ , increases as the fourth power of oxide thickness [15]. For high dose rates and thick oxides, only the initial part of the charge that transports quickly in the CTRW model can reach the interface. In that region, corresponding to 10-15% of the total charge, the slope is nearly flat, and we can consider that the product ηt is constant. Our data at 0 and -25°C fall in that region; shifts in the reference time, τ , at room temperature to lower values will have little effect on the net damage. This explains the essentially flat dependence of the (extrapolated) damage at one second in that temperature regime.

The other limiting case occurs when the irradiation time is much longer than τ , corresponding to effects in thinner oxides or tests at very low dose rates, shown by the shaded region to the right of the figure.

For time scales between these limits, the observed damage will depend on dose rate (or, in the sense of general equivalence, temperature). To some degree, damage depends on the total irradiation time, particularly at the beginning of a long irradiation [16]. However, that dependence will level off if the total irradiation time is longer than approximately 1000τ . First, we need to note that the experiments leading to the CTRW model were done with relatively short pulses from a linear accelerator. Although the entire oxide was flooded with excess electron-hole pairs during the irradiation, the irradiation time was quite short compared to the 1000 s time period over which measurements were done. The conditions under which the transport was measured are

reasonably approximated by our tests at -25°C (as evidenced by the buildup of charge long after irradiation), but not at higher temperatures.

To deal with the case where the irradiation time extends to longer time intervals, we will divide the irradiation into equal time segments, and assume that the CTRW model can be applied to each successive time interval, summing the results of n intervals to obtain the final result for longer irradiations. This is shown pictorially in Fig. 15. The increase in damage results from the fact that the irradiation persists for longer times, extending to the region where the slope of the CTRW transport curve is higher. The average excess electron density is lower compared to an irradiation to the same final dose with a narrower pulse width, decreasing the effect of recombination.

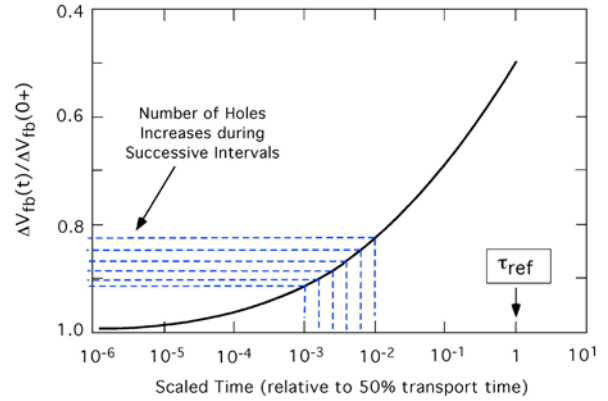


Fig. 15. Increased damage from the recombination model near the “knee” region of the CTRW shape function.

V. CONCLUSIONS

This paper has investigated new features of the ELDRS phenomenon that have not been observed previously. Damage was investigated at much higher dose rates, using a novel experimental method that allows measurements to be made with a single 20 ms pulse, with minimal effect on bias conditions. Damage continues to decrease at dose rates above the 100 rad(SiO_2)/s range, the typical upper limit of most high dose-rate work, extending experimental work into the high carrier density region that was modeled by Boch, *et al.* [14].

Annealing of a significant part of the damage at room temperature is a new, unexpected result that affects testing methods at high dose rate, and may cause uncertainties in the damage observed at higher dose rate. Annealing occurs for parts that are unbiased during irradiation and during the annealing time, as well as for parts that are biased during both phases. Existing total dose test standards need to be modified to take this into account, applying more rigid limits to the time allowed between irradiation and measurement, as well as the time between successive irradiations.

Finally, tests at low temperature showed a long delay time, up to 3,000 seconds, between the peak of the damage and the end of the radiation pulse. This is consistent with older results for MOS gate oxides from the CTRW model for hole transport, using the accepted factors for increased gate oxide thickness. The basic features of the ELDRS effect – the factor of 6 to 8 increase in damage, the difference in the behavior of npn and pnp transistors, and the increased damage under a given set of conditions at elevated temperature – are all consistent with the shape factor predicted by the model.

REFERENCES

- [1] E. W. Enlow, *et al.*, “Response of Advanced Bipolar Processes to Ionizing Radiation,” *IEEE Trans. Nucl. Sci.*, **38**(6), pp. 1342-1351 (1991).
- [2] R. L. Pease, *et al.*, “A Compendium of Recent Total Dose Data on Bipolar Linear Microcircuits,” 1996 IEEE Radiation Effects Data Workshop Record, pp. 28-37.
- [3] T. Carriere, *et al.*, “Evaluation of Accelerated Total Dose Testing of Linear Bipolar Circuits,” *IEEE Trans. Nucl. Sci.*, **47**(6), pp. 2350-2357 (2000).
- [4] T. L. Turflinger, *et al.*, “ELDRS in Space: An Updated and Expanded Analysis of the Bipolar ELDRS Experiment on MPTB,” *IEEE Trans. Nucl. Sci.*, **50**(6), pp. 2328-2334 (2003).
- [5] R. L. Pease, “Total Ionizing Dose Effects in Bipolar Devices and Circuits,” *IEEE Trans. Nucl. Sci.*, **50**(3), pp. 539-551 (2003).
- [6] A. H. Johnston, C. I. Lee and B. G. Rax, “Enhanced Damage in Bipolar Devices at Low Dose Rates: Effects at Very Low Dose Rates,” *IEEE Trans. Nucl. Sci.*, **43**(6), pp. 3049-3059 (1996).
- [7] A. H. Johnston and B. G. Rax, “Failure Modes and Hardness Assurance for Linear Circuits in Space Applications,” *IEEE Trans. Nucl. Sci.*, **57**(4), pp. 1966-1972 (2010).
- [8] T. R. Oldham, *Ionizing Radiation Effects in MOS Oxides*, World Scientific: Singapore(1999).
- [9] G. F. Derbenwick and H. H. Sander, “CMOS Hardness Prediction for Low Dose-Rate Environments,” *IEEE Trans Nucl. Sci.*, **14**(6), pp. 2244-2247 (1977).
- [10] F. B. McLean, H. E. Boesch, Jr., and J. M. McGarrity, *The Physics of SiO₂ and Its Interfaces*, S. T. Pantelides (Ed.), Pergamon Press: New York (1978).
- [11] F. B. McLean, H. E. Boesch, Jr., and J. M. McGarrity, “Hole Transport and Recovery Characteristics of SiO₂ Gate Insulators,” *IEEE Trans. Nucl. Sci.*, **23**(6), pp. 1506-1512 (1976).
- [12] H. E. Boesch, Jr., and F. B. McLean, “Hole Transport in Field Oxides,” *IEEE Trans. Nucl. Sci.*, **32**(6), pp. 3946-3954 (1985).
- [13] R. L. Pease, R. D. Schrimpf and D. M. Fleetwood, “ELDRS in Bipolar Linear Circuits: A Review”, *IEEE Trans. Nucl. Sci.*, **56**(4), pp. 1894-1908 (2009).
- [14] J. Boch, *et al.*, “Physical Model for the Low-Dose-Rate Effect in Bipolar Devices,” *IEEE Trans. Nucl. Sci.*, **53**(6), pp. 3635-3660 (2006).
- [15] T. R. Oldham and F. B. McLean, “Total Ionizing Dose Effects in MOS Oxides and Devices,” *IEEE Trans. Nucl. Sci.*, **50**(3), pp. 483-499 (2003).
- [16] R. K. Freitag and D. B. Brown, “Low Dose Rate Effects on Bipolar IC’s: Experiments on the Time Dependence”, *IEEE Trans. Nucl. Sci.*, **44**(6), pp. 1906-1913 (1997).